ISSN 0915-633X

NATIONAL INSTITUTE FOR FUSION SCIENCE

Fast Potential Change in Sawteeth in JIPP T-IIU Tokamak Plasmas

Y. Hamada, A. Nishizawa, Y. Kawasumi, K. Kawahata, K. Itoh, A. Ejiri, K. Toi, K. Narihara, K. Sato, T. Seki, H. Iguchi, A. Fujisawa, K. Adachi, S. Hidekuma, S. Hirokura, K. Ida, M. Kojima, J. Koong, R. Kumazawa, H. Kuramoto, R. Liang, T. Minami, H. Sakakita, M. Sasao, K.N. Sato, T. Tsuzuki, J. Xu, I. Yamada, T. Watari

(Received - Nov. 25, 1994)

NIFS-327 Dec. 1994

RESEARCH REPORT
NIFS Series

NAGOYA, JAPAN

Fast Potential Change in Sawteeth in JIPP T-IIU Tokamak Plasmas

Y.Hamada, A.Nishizawa, Y.Kawasumi, K.Kawahata, K.Itoh, A.Ejiri, K.Toi, K.Narihara, K.Sato, T.Seki, H.Iguchi, A.Fujisawa, K.Adachi, S.Hidekuma, S.Hirokura, K.Ida, M.Kojima, J.Koong, R.Kumazawa, H.Kuramoto, R.Liang, T.Minami, H.Sakakita, M.Sasao, K.N.Sato, T.Tsuzuki, J.Xu, I.Yamada, T.Watari

National Institute for Fusion Science

Nagoya, 464-01, Japan

Fast changes of electric potential with different polarities are observed during sawtooth oscillation in a core region of a tokamak plasma using a heavy ion beam probe. The potential change inside the inversion radius is found to be positive. The change is negative outside the inversion radius and shows clearly a propagation nature. The observed potential can be interpreted by the mixture of the potentials of two origins. One of them drives the fast MHD plasma motion through E/B drift and the other is a barrier potential induced by mixing of hot and cold plasmas at sawtooth crash.

Keywords: sawtooth oscillation, tokamak, electric potential, HIBP, ECE.

A periodic crash of the central electron temperature called sawtooth oscillation is a common feature of tokamak plasmas.[1-6] After the crash, the flattening of the pressure throughout the q=1 surface is observed. Kadomtsev proposed a theoretical model of the resistive reconnection.[7] The theory predicted the flattening of the q-profile as well as the pressure profile inside the q=1 surface. The prediction was, however, found to be in contradiction with the recent measurement of the current density in tokamak plasmas.[8] In addition, the experiment in large machines such as JET and TFTR showed much faster crashes than the prediction by the resistive reconnection.[3,4,5] More refined theories taking account of the kinetic effect and ergodicity on the reconnections, are now proposed.[9,10] In this paper, we report the first measurement of potential changes during sawtooth oscillations and discuss the implications of the results.

The experiment is performed at JIPP T-IIU tokamak.[11] Major radius is 93 cm and the maximum toroidal field is 3 Tesla. The experiment is conducted at a relatively low electron density of about $2 \times 10^{13}/cm^3$ for good beam penetration into the center of the plasma. The thallium ion beam with the energy of 450 keV is injected into the tokamak as a heavy ion beam probing (HIBP).[12,13,14] The HIBP setup is similar to that in

TEXT tokamak[15]. Intensity and change of energy of the secondary beam (Tl^{++}) produced in a tokamak plasma are measured by a parallel-plate analyzer in order to study the local density and the local potential.

The basic principle of the potential measurement by HIBP was proposed by R.L.Hickok et al.[16] and is illustrated in Fig.1a. The amount of the change in a total kinetic energy of the secondary beam detected at an energy analyzer is the local plasma potential where the ionization of a primary beam takes place, if the change of the beam energy due to the electric field caused by the time derivative of a vector potential $d\mathbf{A}/dt$, is negligible. Since in low-ß plasmas like tokamak plasmas, perturbed $\mathbf{A}$ is parallel to an equilibrium magnetic field[17] and is nearly perpendicular to the trajectory of the probing beam in our experiment. It does not, therefore, affect the beam energy. The change in the beam energy even in the MHD time scale is due to an electrostatic potential at the ionization point. The current-profile change induces, however, the change of a toroidal deflection angle and an out-of-plane entrance angle ($\delta\omega_{en}$) to the analyzer. Since a parallel-plate analyzer measures the energy of the movement parallel to the analyzer plane (the plane of symmetry of the analyzer) instead of a total kinetic energy, the current-profile change causes the error of $-\delta\{V_b \sin^2(\omega_{en})\} = -2V_b \sin(\omega_{en,o})\cos(\omega_{en,o})\delta\omega_{en}$ in the potential measurement,[13,14] where V_b is the primary beam energy and $\omega_{en,o}$ is the out-of entrance angle before the crash. Since this error changes sign as $\omega_{en,o}$ changes sign, we can estimate the magnitude of this error by conducting the measurements at various values of $\omega_{en,o}$ through changing the toroidal angle of the analyzer plane.

The birth place of the secondary ions Tl^{++} that go out of the plasma and pass through an input slit of the energy analyzer, is the point of measurement (sample volume). It can be swept across a plasma cross-section by sweeping an injection angle to the tokamak as shown in Fig.1b. A small change of the energy is measured by the parallel-plate analyzer in terms of the normalized difference (ND) of secondary beam currents to upper and lower detector plates (I_u, I_d), where, ND=$(I_u-I_d)/(I_u+I_d)$.[13,14,16] The conversion rate of ND to plasma potential is about 1 kV/ND in the case of 450 keV beam. Figure 1b shows trajectories of 450 kV thallium beams at the toroidal field of 3 Tesla and points of measurement (sample volume A, B and C) in this experiment. A 10-channel ECE polychromator and 8-channel x-ray pin-diode horizontal arrays are used for the study of sawtooth oscillation. Because of a relatively small number of detectors of ECE and soft x-ray a tomographic analysis of the change in magnetic configurations inside the q=1 surface is rather difficult.

Figure 2 shows typical fast changes of the potential at A, B and C shown in Fig.1b. Plasma current is about 220 kA (q_a = 4.5), and in order to increase the inversion radius, an additional heating by IBW or NBI is performed. In Fig.2a, very sharp positive changes are observed at A in Fig.1b, well inside the inversion layer of ECE and soft x-ray. At B, near the inversion layer, mixtures of positive and negative potential pulse are observed as shown in Fig.2b. At C, outside the inversion radius, negative potential pulses are observed in Fig.2c. In order to check how ND is affected by the beam deflection due to the current-profile change at sawtooth, we measured ND under various out-of-plane entrance angles by changing the analyzer plane toroidally. Since the same characteristics of fast changes at sawtooth oscillation were obtained, we can conclude that the current-profile change at the sawtooth crash does not contribute much to the change of ND and the change of ND records the change of the local plasma potential.

We found by ECE and x-ray measurements that the polarity of fast potential changes in Fig.2b (near the inversion layer) depends on the direction of the fast movement[3,5,6)] of a hot core just before a rapid decay of the electron temperature. Figure 3 shows expanded views of the plasma potential at B, and signals of 3 sawtoothing ECE channels. Horizontal (radial) movements of the hot core can be measured by ECE measurement if we assume an n=1/m=1 structure of the perturbation. Before sawtooth crashes, n=1/m=1 oscillations are observed to grow. During the n=1/m=1 oscillations, a radial (outwards) fast movement of the hot core is observed in the case of Fig.3a. In this case a negative change of the potential is observed. In Fig.3b, the movement of the hot core is inwards and a positive potential pulse is observed. We can conclude that if a fast adiabatic movement of the hot core before the crash is towards the point of measurement, the potential change is positive and vice versa, taking into consideration that the ECE and HIBP measurements are separated toroidally by 120 degrees. Since the pulse length of a fast potential change is about 1/3 of the period of the n=1/m=1 oscillation, a potential pulse at B is modulated by the oscillation and is often followed by a pulse of different polarity depending on the angle of the adiabatic motion, as shown in Fig.3b.

In reduced MHD equations plasma motion perpendicular to the magnetic field $\mathbf{v}_\perp$, is described by Φ_{MHD} through $\mathbf{v}_\perp = \mathbf{E}\times\mathbf{B}/B^2$ where $\mathbf{E} = -\nabla\Phi_{MHD}$. In a sawtooth crash, the theories predict the potential which causes rather uniform shift inside the q=1 surface.[7,10,17] The maximum MHD potential Φ_{MHD} occurs near the inversion radius and may be estimated by the $\Phi_{MHD} = v_\perp \times B_t \times r_{inv}$. At the fast adiabatic motion just before the crash at Fig.3b, the estimated maximum potential is $\Phi_{MHD} = \sim 100$eV. The experimentally observed potential at the adiabatic shift is in rough agreement in magnitude and polarity although it is complicated because of the n=1/m=1 oscillation. In case of Fig.3a, the adiabatic shift is slow and the observed potential is small in accordance with Φ_{MHD}. The observed potential reaches, however, its peak where the crash is completed and there is presumably no MHD motion. In addition, the predicted MHD potential near the magnetic axis may be small and change its polarity depending on the direction of the fast movement in contradiction with the observed behaviour at A. Accordingly, we conclude that observed fast changes of a potential are the mixtures of a MHD potential Φ_{MHD} and a transient ambipolar potential along the magnetic line of force (barrier potential), caused by the mixing of a hot core inside the q=1 surface with a cold plasma through the reconnection or enhanced ergodicity at the crash.

The larger number of electrons of the hotter and denser plasma diffuse through destroyed magnetic surfaces into the region of cold plasma, changing a local space potential (formation of barrier potential). The region of higher pressure (A) will become positive and cold region (C) will be negative in accordance with experimental results. The predicted MHD potential is small and the observed potential is dominated by the barrier potential at both regions. This is the effect which can not be predicted by the one-fluid-reduced-MHD equations.

The change of the potential during the intervals of crashes shown in Fig.2 is small compared with the fast potential changes. This means that the potential profile inside the q=1 surface is rather flat and the observed fast change of the potential is not due to the mixing of the plasmas with different space potentials at the sawtooth crashes. The formation of a large change of a space potential along a magnetic line of force in different plasmas separated by magnetic mirrors, plug or thermal barrier potential, is the target of intensive researches in mirror confinement experiment.[20] This experiment is the first observation of a change of space potential due to the interaction of plasmas with different pressures in a torus experiment, where the mirror ratio is very small. The formation of an electrostatic potential barrier in plasmas with different pressures buried in the uniform magnetic field was observed at a linear steady-state plasma experiment.[21] The polarities of the potential agree with our results. The maximum change of the potential after the crash (barrier potential) is about 100-200 V and is approximately the same with the change of the electron temperature measured by YAG Thomson scattering and ECE measurement; $T_{e,YAG}(0) = 1.2$ keV and $\Delta T_{e,ECE}(0)/T_{e,ECE}(0) = 0.1$. Since the observed potential barrier is small compared to the electron temperature, the effect of this barrier potential on an electron heat flow may be small in these low-density plasmas. If the plasma density is higher and the density peaking is larger, the barrier potential may be dominated by the difference of the densities across the inversion layer and the potential difference may be order of the electron temperature, producing large effect on a heat flow at the crashes.

The fact that the change of a space potential near the center of the plasma (A) is always positive as shown in Fig.2a means that A belongs to a hot core and a flow of electrons and energy from the hot core continues during the crash. B belongs to the island (reconnected area) in the case of Fig.3a or belongs to the hot core (Fig.3b), depending on the direction of the fast movement of a hot core. If the total reconnection of magnetic surfaces predicted by B.B.Kadomtsev[7] occurs, A will belong to a reconnected area at the final stage of the decay and the observed potential will be negative, since A is near the plasma center. The positive change of potential at A suggests that the magnetic configurations continue to be displaced nested surfaces with an island and A stays in a core region during the whole decay of the temperature. The same conclusion was obtained in the detailed tomographic study of the sawtooth in WT-3 tokamak.[6] This was also suggested in the observation of the small change in q profiles before and after the sawtooth oscillations.[8] The rapid heat flow in sawtooth may be caused by the enhanced ergodization suggested by A. J. Lichtenberg et al.[9] These fast changes in potential are observed in OH, NBI-heated and IBW-heated plasmas.

Figure 4 shows expanded views of a plasma potential and the ECE signal at the plasma center, when the sample volume is outside the inversion layer, (C). The potential change shows a clear delay time and a sharp fall in contrast to the diffusive natures[22] of the ECE and soft x-ray signals in sawtooth propagation. The magnitude of the delay time in potential change is similar to the ECE measurement in sawteeth propagation as shown in Fig. 5. The reason for a sharp fall in the potential is not clear and a detailed study is impeded by the noise of the signals due to the ripple of the analyzer voltage.

The potential signal in Fig.4 shows no change at the time of crash of ECE signals in the center. The trajectory of the secondary beam of C, crosses the inversion layer and may be influenced by the change of the vector potential $d\mathbf{A}/dt$. This result, therefore, shows that the influence of $d\mathbf{A}/dt$ on the potential measurement is negligible.

In summary, a fast potential change is observed at sawtooth crash and explained by the mixture of a fast potential which drives the rapid plasma motion and a barrier potential by the mixing of hot and cold plasmas. The observed potential change near the axis is comparable to the change of the electron temperature at the crash and may not have a significant effect on the heat flow in this experiment. Its effect may be large in the plasma where the density peaking is significant and the difference of the plasma density across the inversion layer is large. The detailed study suggests the partial reconnection and the enhanced ergodization of the magnetic surface during the crashes.

We would like to thank to Director-General of our institute, A. Iiyoshi and Professors M. Fujiwara and K.Matsuoka for their continuous supports. We aknowledge useful discussions with Prof. J. Todoroki.

Reference

1) S.von Goeler,W.Stodiek, and N.Sauthoff, Phys. Rev. Letts.**33** 1201 (1974).

2) M.A.Dubois,A.L.Pecquet,C.Reverdin, Nuclear Fusion **23** (1983) 147.

3) A.W.Edwards et al.,Phys. Rev. Letts. **57** 210 (1986).

4) D.J.Campbel et al.,Nuclear Fusion **26** (1986) 1085.

5) Y.Nagayama et al.,Phys. Rev. Letts. **67** 3527 (1991).

6) K.Hanada, J. Phys.Soc.Japan **63** 967 (1994).

7) B.B.Kadomtsev, Fiz.Plazmy **1** 710 (1975). [Sov.J.Plasma Phys. **1** 389 (1975)].

8) H.Soltwisch,W.Stodiek,J.Manickam,and J.Schluter,*Proc. 11th Int. Conf. on Plasma Physics and Conrolled Nuclear Fusion Research,Kyoto,*IAEA, Vienna, Vol.1, p.263(1987).

9) A.J.Lichtenberg,K.Itoh,S.-I.Itoh,A.Fukuyama,Nuclear Fusion **32** (1992) 495.

10)A.Y.Aydemir, Phys. Fluids B **4** 3471 (1992).

11) K.Toi, et al., *Proc.13th Int. Conf. on Plasma Physics and Conrolled Nuclear Fusion Research, Washington, D.C.*, IAEA, Vienna, Vol.1, p.301 (1991).

12) Y.Hamada, Y.Kawasumi, M.Masai, H.Iguchi, A.Fujisawa and JIPP T-11U Group, Annual Review of NIFS, p.118 (1990).

13) Y.Hamada et al., J. Plasma Fusion Res. **69** 1050 (1993).

14) Y.Hamada et al., Plasma Phys. Control. Fusion **36** 1743 (1994).

15) P.M.Schoch, J.C.Forster, W.C.Jennings, and R.L.Hickok, Rev. Sci. Instrum. **57** 1825 (1986).

16) J.C.Jobes, and R.L.Hickok, Nuclear Fusion **10** 195 (1970)

17) for example, B.B.Kadomtsev and O.P.Pogutse, in Rev.of Plasma Physics, Consultants Bureau, (1970) N.Y.vol.5 p.284.

18) L.Solensten and K.A.Connor, Rev.Sci.Instrum.**58** 516 (1987).

19) D.Biskamp, Phys.Fluids B**3** 3353 (1991).

20) For example, M.Inutake et al., *Proc. 14th Int. Conf. on Plasma Physics and Conrolled Nuclear Fusion Research, Wurzburg,* IAEA, Vienna, Vol.12, p.651 (1992).

21) R.Hatakeyama, Y.Suzuki and N.Sato,, Phys. Rev. Letts.**50** 1203 (1983).

22) J.D.Callen, G.L.Jahns, Phys. Rev. Letts. **38** 491 (1977).

Figure Captions

Figure 1. a) Basic principle of potential measurement in the plasma by a heavy ion beam probe. If the electric field is purely electrostatic, the change in the secondary beam energy coincides with the local plasma potential at the place where the ionization takes place. r_x in the figure is the place where the ionization takes place . b) Trajectories of primary and secondary beam detected by the analyzer. Positions of the sample volumes A,B and C and sawtooth inversion circle are also shown.

Figure 2. Typical changes of ND (the difference of the upper and lower detector currents, normalized by the sum) at three positions of sample volumes (A,B and C on Fig.1b) . r_{inv} is the sawtooth inversion radius. Figure 2a, 2b and 2c correspnd to A, B, and C respectively. The conversion ratio from ND to the change in the plasma potential is about 1 kV/ND. Also the enlarged signals of the central ECE emission are shown for reference.

Figure 3. The expanded views of ND (potential) of Fig.2b and signals of 3 positively sawtoothing ECE channels at sample volume B near the inverison radius. Vertical scales of ECE signals are in arbitrary unit. (a) Case of a negative potential change. (b) Case of a positive potential change.

Figure 4. The expanded time behaviours of ND, (a) and ECE center channel (b), in case of Fig.2c showing the propagating nature of the potential pulse.

Figure 5. Delay time of the potential pulse to the decay of the center ECE channel at the crash as shown in Fig. 4, versus position of sample volume. + shows the delay time observed by ECE signal.

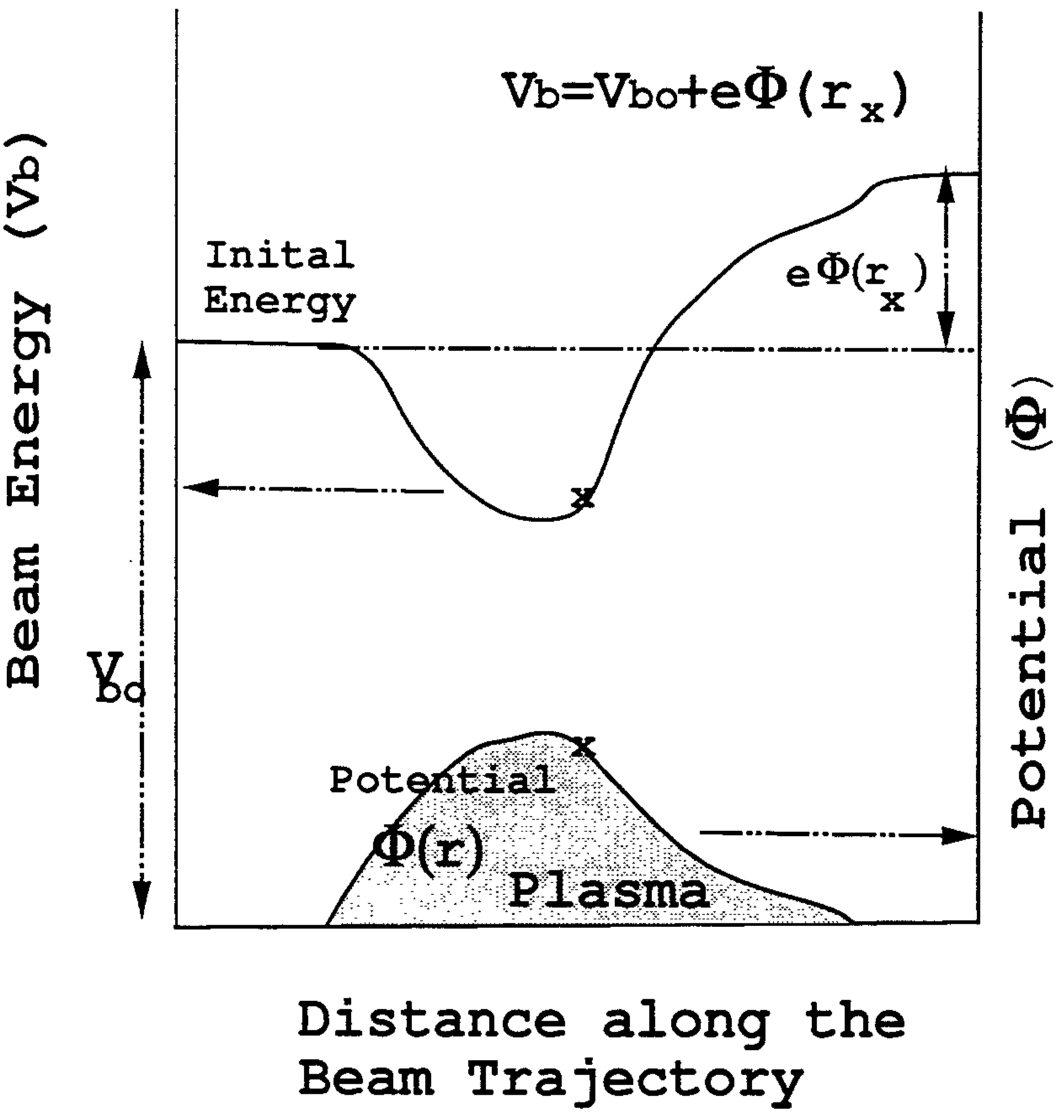

Vb=Vbo+eΦ(r x)
Inital
Energy
eΦ(r x)
Beam Energy (Vb)
Vbo
x
x
Potential
Φ(r)
Plasma
Potential (Φ)
Distance along the
Beam Trajectory

Fig.1a

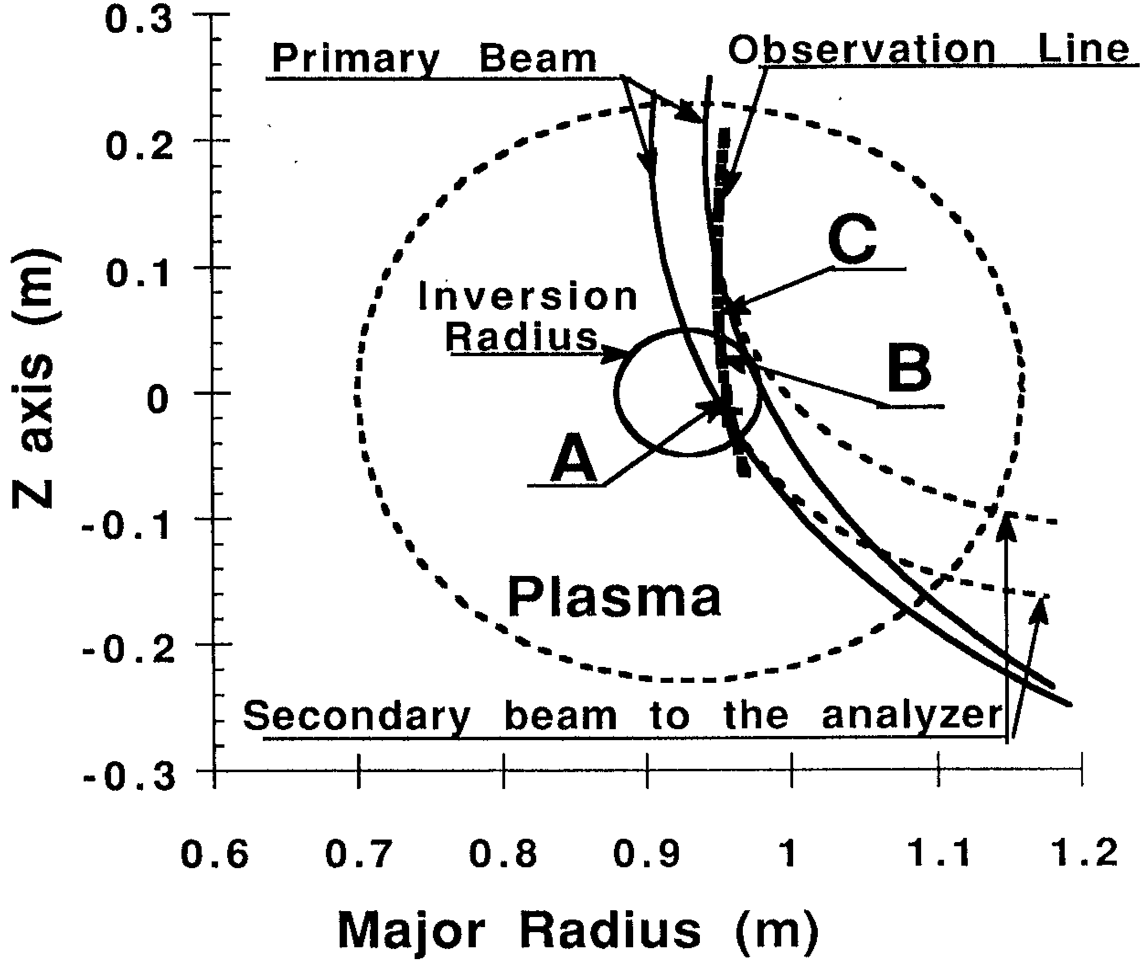
0.3
0.2
0.1
0
-0.1
-0.2
-0.3
Z axis (m)
Primary Beam
Observation Line
C
Inversion
Radius
B
A
Plasma
Secondary beam to the analyzer
0.6
0.7
0.8
0.9
1
1.1
1.2
Major Radius (m)

Fig.1b

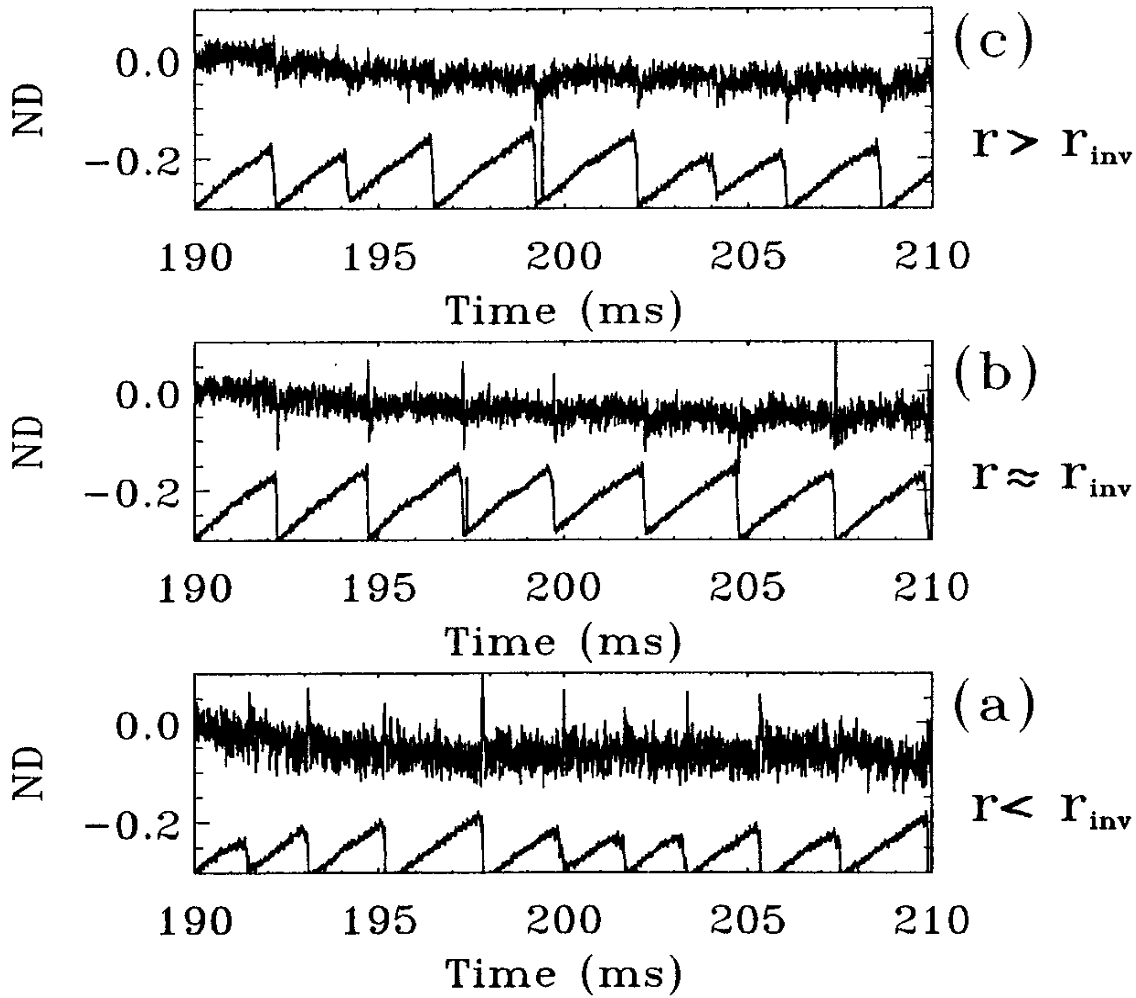
(c)
$r > r_{inv}$
(b)
$r \approx r_{inv}$
(a)
$r < r_{inv}$
ND
0.0
−0.2
190
195
200
205
210
Time (ms)

Fig.2

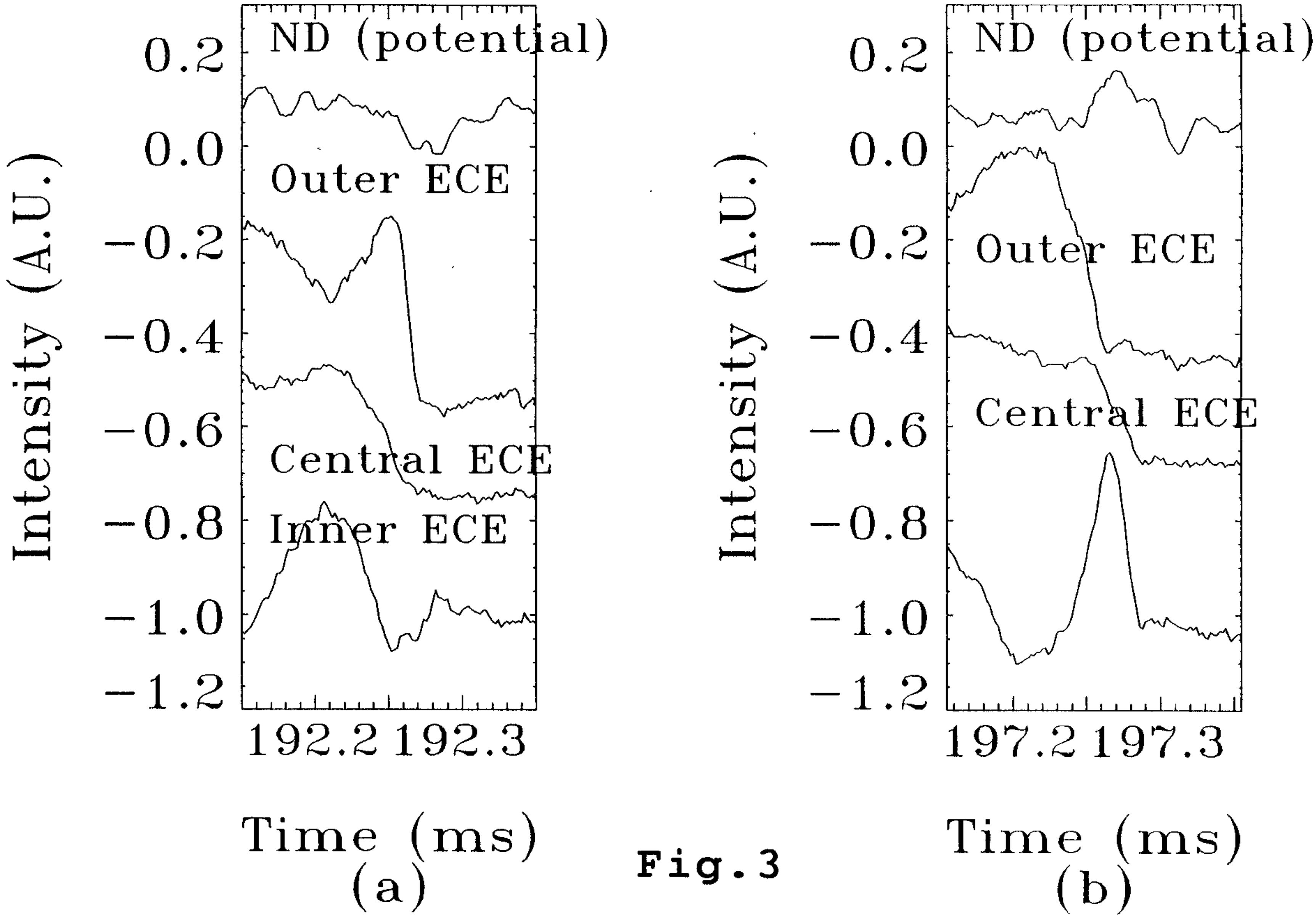
ND (potential)
Outer ECE
Central ECE
Inner ECE
Intensity (A.U.)
0.2
0.0
−0.2
−0.4
−0.6
−0.8
−1.0
−1.2
192.2
192.3
Time (ms)
ND (potential)
Outer ECE
Central ECE
Intensity (A.U.)
197.2
197.3
Time (ms)

(a) (b)

Fig.3

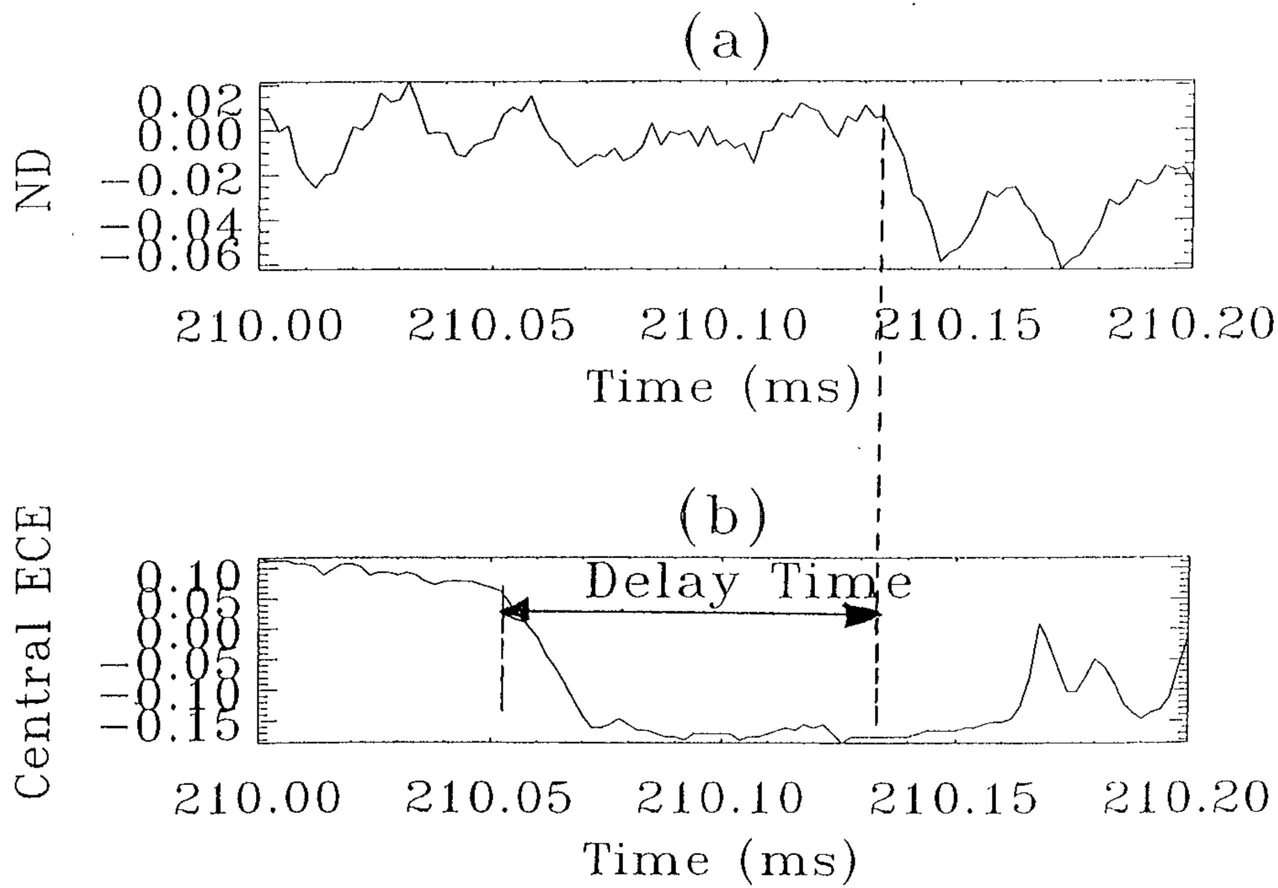
(a)
ND
0.02
0.00
-0.02
-0.04
-0.06
210.00
210.05
210.10
210.15
210.20
Time (ms)
(b)
Central ECE
Delay Time
0.10
0.05
0.00
-0.05
-0.10
-0.15
210.00
210.05
210.10
210.15
210.20
Time (ms)

Fig.4

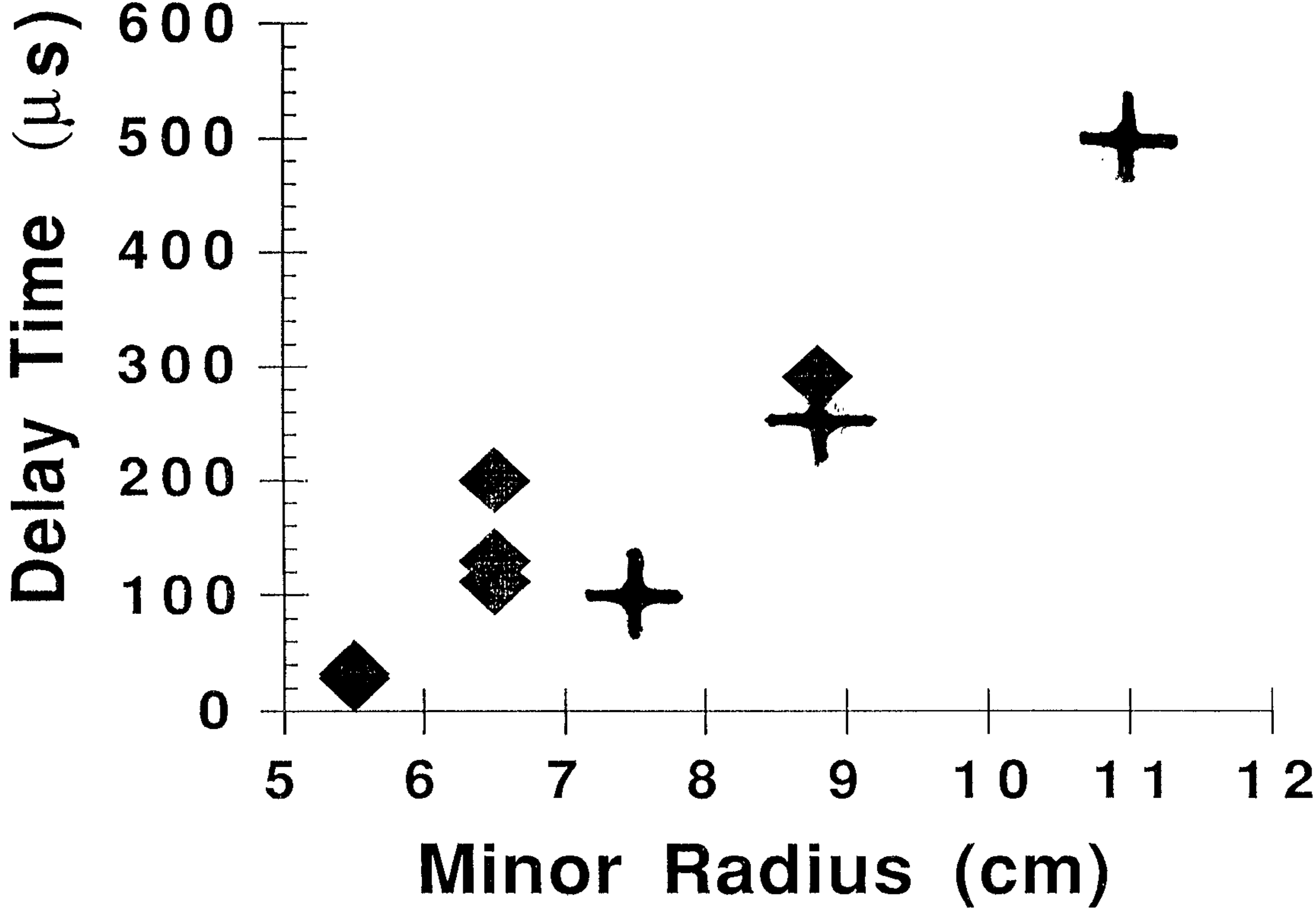
Delay Time (μs)
600
500
400
300
200
100
0
5
6
7
8
9
10
11
12
Minor Radius (cm)

Fig.5

Recent Issues of NIFS Series

NIFS-286 H. Sanuki, K. Itoh, J. Todoroki, K. Ida, H. Idei, H. Iguchi and H. Yamada,
Theoretical and Experimental Studies on Electric Field and Confinement in Helical Systems; June 1994

NIFS-287 K. Itoh and S-I. Itoh,
Influence of the Wall Material on the H-mode Performance; June 1994

NIFS-288 K. Itoh, A. Fukuyama, S.-I. Itoh, M. Yagi and M. Azumi,
Self-Sustained Magnetic Braiding in Toroidal Plasmas: July 1994

NIFS-289 Y. Nejoh,
Relativistic Effects on Large Amplitude Nonlinear Langmuir Waves in a Two-Fluid Plasma; July 1994

NIFS-290 N. Ohyabu, A. Komori, K. Akaishi, N. Inoue, Y. Kubota, A.I. Livshit, N. Noda, A. Sagara, H. Suzuki, T. Watanabe, O. Motojima, M. Fujiwara, A. Iiyoshi,
Innovative Divertor Concepts for LHD; July 1994

NIFS-291 H. Idei, K. Ida, H. Sanuki, S. Kubo, H. Yamada, H. Iguchi, S. Morita, S. Okamura, R. Akiyama, H. Arimoto, K. Matsuoka, K. Nishimura, K. Ohkubo, C. Takahashi, Y. Takita, K. Toi, K. Tsumori and I. Yamada,
Formation of Positive Radial Electric Field by Electron Cyclotron Heating in Compact Helical System; July 1994

NIFS-292 N. Noda, A. Sagara, H. Yamada, Y. Kubota, N. Inoue, K. Akaishi, O. Motojima, K. Iwamoto, M. Hashiba, I. Fujita, T. Hino, T. Yamashina, K. Okazaki, J. Rice, M. Yamage, H. Toyoda and H. Sugai,
Boronization Study for Application to Large Helical Device; July 1994

NIFS-293 Y. Ueda, T. Tanabe, V. Philipps, L. Könen, A. Pospieszczyk, U. Samm, B. Schweer, B. Unterberg, M. Wada, N. Hawkes and N. Noda,
Effects of Impurities Released from High Z Test Limiter on Plasma Performance in TEXTOR; July. 1994

NIFS-294 K. Akaishi, Y. Kubota, K. Ezaki and O. Motojima,
Experimental Study on Scaling Law of Outgassing Rate with A Pumping Parameter, Aug. 1994

NIFS-295 S. Bazdenkov, T. Sato, R. Horiuchi, K. Watanabe,
Magnetic Mirror Effect as a Trigger of Collisionless Magnetic Reconnection, Aug. 1994

NIFS-296 K. Itoh, M. Yagi, S.-I. Itoh, A. Fukuyama, H. Sanuki, M. Azumi,

Anomalous Transport Theory for Toroidal Helical Plasmas,
Aug. 1994 (IAEA-CN-60/D-III-3)

NIFS-297 J. Yamamoto, O. Motojima, T. Mito, K. Takahata, N. Yanagi, S. Yamada, H. Chikaraishi, S. Imagawa, A. Iwamoto, H. Kaneko, A. Nishimura, S. Satoh, T. Satow, H. Tamura, S. Yamaguchi, K. Yamazaki, M. Fujiwara, A. Iiyoshi and LHD group,
New Evaluation Method of Superconductor Characteristics for Realizing the Large Helical Device; Aug. 1994 (IAEA-CN-60/F-P-3)

NIFS-298 A. Komori, N. Ohyabu, T. Watanabe, H. Suzuki, A. Sagara, N. Noda, K. Akaishi, N. Inoue, Y. Kubota, O Motojima, M. Fujiwara and A. Iiyoshi,
Local Island Divertor Concept for LHD; Aug. 1994 (IAEA-CN-60/F-P-4)

NIFS-299 K. Toi, T. Morisaki, S. Sakakibara, A. Ejiri, H. Yamada, S. Morita, K. Tanaka, N. Nakajima, S. Okamura, H. Iguchi, K. Ida, K. Tsumori, S. Ohdachi, K. Nishimura, K. Matsuoka, J. Xu, I. Yamada, T. Minami, K. Narihara, R. Akiyama, A. Ando, H. Arimoto, A. Fujisawa, M. Fujiwara, H. Idei, O. Kaneko, K. Kawahata, A. Komori, S. Kubo, R. Kumazawa, T. Ozaki, A. Sagara, C. Takahashi, Y. Takita and T. Watari,
Impact of Rotational-Transform Profile Control on Plasma Confinement and Stability in CHS; Aug. 1994 (IAEA-CN-60/A6/C-P-3)

NIFS-300 H. Sugama and W. Horton,
Dynamical Model of Pressure-Gradient-Driven Turbulence and Shear Flow Generation in L-H Transition; Aug. 1994 (IAEA/CN-60/D-P-I-11)

NIFS-301 Y. Hamada, A. Nishizawa, Y. Kawasumi, K.N. Sato, H. Sakakita, R. Liang, K. Kawahata, A. Ejiri, K. Narihara, K. Sato, T. Seki, K. Toi, K. Itoh, H. Iguchi, A. Fujisawa, K. Adachi, S. Hidekuma, S. Hirokura, K. Ida, M. Kojima, J. Koog, R. Kumazawa, H. Kuramoto, T. Minami, I. Negi, S. Ohdachi, M. Sasao, T. Tsuzuki, J. Xu, I. Yamada, T. Watari,
Study of Turbulence and Plasma Potential in JIPP T-IIU Tokamak;
Aug. 1994 (IAEA/CN-60/A-2-III-5)

NIFS-302 K. Nishimura, R. Kumazawa, T. Mutoh, T. Watari, T. Seki, A. Ando, S. Masuda, F. Shinpo, S. Murakami, S. Okamura, H. Yamada, K. Matsuoka, S. Morita, T. Ozaki, K. Ida, H. Iguchi, I. Yamada, A. Ejiri, H. Idei, S. Muto, K. Tanaka, J. Xu, R. Akiyama, H. Arimoto, M. Isobe, M. Iwase, O. Kaneko, S. Kubo, T. Kawamoto, A. Lazaros, T. Morisaki, S. Sakakibara, Y. Takita, C. Takahashi and K. Tsumori,
ICRF Heating in CHS; Sep. 1994 (IAEA-CN-60/A-6-I-4)

NIFS-303 S. Okamura, K. Matsuoka, K. Nishimura, K. Tsumori, R. Akiyama, S. Sakakibara, H. Yamada, S. Morita, T. Morisaki, N. Nakajima, K. Tanaka, J. Xu, K. Ida, H. Iguchi, A. Lazaros, T. Ozaki, H. Arimoto, A. Ejiri, M. Fujiwara, H. Idei, A. Iiyoshi, O, Kaneko, K. Kawahata, T. Kawamoto, S. Kubo, T. Kuroda, O. Motojima, V.D. Pustovitov, A. Sagara, C. Takahashi,

K. Toi and I. Yamada,
High Beta Experiments in CHS; Sep. 1994 (IAEA-CN-60/A-2-IV-3)

NIFS-304 K. Ida, H. Idei, H. Sanuki, K. Itoh, J. Xu, S. Hidekuma, K. Kondo, A. Sahara, H. Zushi, S.-I. Itoh, A. Fukuyama, K. Adati, R. Akiyama, S. Bessho, A. Ejiri, A. Fujisawa, M. Fujiwara, Y. Hamada, S. Hirokura, H. Iguchi, O. Kaneko, K. Kawahata, Y. Kawasumi, M. Kojima, S. Kubo, H. Kuramoto, A. Lazaros, R. Liang, K. Matsuoka, T. Minami, T. Mizuuchi, T. Morisaki, S. Morita, K. Nagasaki, K. Narihara, K. Nishimura, A. Nishizawa, T. Obiki, H. Okada, S. Okamura, T. Ozaki, S. Sakakibara, H. Sakakita, A. Sagara, F. Sano, M. Sasao, K. Sato, K.N. Sato, T. Saeki, S. Sudo, C. Takahashi, K. Tanaka, K. Tsumori, H.Yamada, I. Yamada, Y. Takita, T. Tuzuki, K. Toi and T. Watari,
Control of Radial Electric Field in Torus Plasma; Sep. 1994 (IAEA-CN-60/A-2-IV-2)

NIFS-305 T. Hayashi, T. Sato, N. Nakajima, K. Ichiguchi, P. Merkel, J. Nührenberg, U. Schwenn, H. Gardner, A. Bhattacharjee and C.C.Hegna,
Behavior of Magnetic Islands in 3D MHD Equilibria of Helical Devices; Sep. 1994 (IAEA-CN-60/D-2-II-4)

NIFS-306 S. Murakami, M. Okamoto, N. Nakajima, K.Y. Watanabe, T. Watari, T. Mutoh, R. Kumazawa and T. Seki,
Monte Carlo Simulation for ICRF Heating in Heliotron/Torsatrons; Sep. 1994 (IAEA-CN-60/D-P-I-14)

NIFS-307 Y. Takeiri, A. Ando, O. Kaneko, Y. Oka, K. Tsumori, R. Akiyama, E. Asano, T. Kawamoto, T. Kuroda, M. Tanaka and H. Kawakami,
Development of an Intense Negative Hydrogen Ion Source with a Wide-Range of External Magnetic Filter Field; Sep. 1994

NIFS-308 T. Hayashi, T. Sato, H.J. Gardner and J.D. Meiss,
Evolution of Magnetic Islands in a Heliac; Sep. 1994

NIFS-309 H. Amo, T. Sato and A. Kageyama,
Intermittent Energy Bursts and Recurrent Topological Change of a Twisting Magnetic Flux Tube; Sep.1994

NIFS-310 T. Yamagishi and H. Sanuki,
Effect of Anomalous Plasma Transport on Radial Electric Field in Torsatron/Heliotron; Sep. 1994

NIFS-311 K. Watanabe, T. Sato and Y. Nakayama,
Current-profile Flattening and Hot Core Shift due to the Nonlinear Development of Resistive Kink Mode; Oct. 1994

NIFS-312 M. Salimullah, B. Dasgupta, K. Watanabe and T. Sato,
Modification and Damping of Alfvén Waves in a Magnetized Dusty

Plasma; Oct. 1994

NIFS-313 K. Ida, Y. Miura, S -I. Itoh, J.V. Hofmann, A. Fukuyama, S. Hidekuma, H. Sanuki, H. Idei, H. Yamada, H. Iguchi, K. Itoh,
Physical Mechanism Determining the Radial Electric Field and its Radial Structure in a Toroidal Plasma; Oct. 1994

NIFS-314 Shao-ping Zhu, R. Horiuchi, T. Sato and The Complexity Simulation Group,
Non-Taylor Magnetohydrodynamic Self-Organization; Oct. 1994

NIFS-315 M. Tanaka,
Collisionless Magnetic Reconnection Associated with Coalescence of Flux Bundles; Nov. 1994

NIFS-316 M. Tanaka,
Macro-EM Particle Simulation Method and A Study of Collisionless Magnetic Reconnection; Nov. 1994

NIFS-317 A. Fujisawa, H. Iguchi, M. Sasao and Y. Hamada,
Second Order Focusing Property of 210° Cylindrical Energy Analyzer; Nov. 1994

NIFS-318 T. Sato and Complexity Simulation Group,
Complexity in Plasma - A Grand View of Self- Organization; Nov. 1994

NIFS-319 Y. Todo, T. Sato, K. Watanabe, T.H. Watanabe and R. Horiuchi,
MHD-Vlasov Simulation of the Toroidal Alfvén Eigenmode; Nov. 1994

NIFS-320 A. Kageyama, T. Sato and The Complexity Simulation Group,
Computer Simulation of a Magnetohydrodynamic Dynamo II: Nov. 1994

NIFS-321 A. Bhattacharjee, T. Hayashi, C.C.Hegna, N. Nakajima and T. Sato,
Theory of Pressure-induced Islands and Self-healing in Three-dimensional Toroidal Magnetohydrodynamic Equilibria; Nov. 1994

NIFS-322 A. Iiyoshi, K. Yamazaki and the LHD Group,
Recent Studies of the Large Helical Device; Nov. 1994

NIFS-323 A. Iiyoshi and K. Yamazaki,
The Next Large Helical Devices; Nov. 1994

NIFS-324 V.D. Pustovitov
Quasisymmetry Equations for Conventional Stellarators; Nov. 1994

NIFS-325 A. Taniike, M. Sasao, Y. Hamada, J. Fujita, M. Wada,
The Energy Broadening Resulting from Electron Stripping Process of a Low Energy Au⁻ Beam; Dec. 1994

NIFS-326 I. Viniar and S. Sudo,
New Pellet Production and Acceleration Technologies for High Speed Pellet Injection System "HIPEL" in Large Helical Device; Dec. 1994